
VI Workshop de Visão Computacional
04-07 Julho/2010 - Presidente Prudente, SP - Brasil
ISSN 2175-6120
FAPESP
SBC
opto
unesp
UNIVERSIDADE ESTADUAL PAULISTA
JÚLIO DE MESQUITA FILHO
ENGEFOTO
CNPq
Fundunesp
CAPES

Condições Climáticas:
Temperatura: 30°C/ 86°F
Umidade: 62%

Home

Home
Local
Programa
Comitês
Tópicos de Interesse
WVC Anteriores
Datas Importantes
Inscrições/Taxas
Submissão de Trabalhos
Parceiros
Apoio aos Participantes
Contatos

Bem-vindos ao site oficial do VI Workshop de Visão Computacional.

A área de Visão Computacional, fortemente consolidada em vários países, tem-se desenvolvido de maneira intensa nos últimos anos, desenvolvimento em grande parte motivado por seu alto poder de geração de novas tecnologias (produtos, processos). No Brasil, essa situação não é diferente, sendo possível observar inúmeros grupos de pesquisadores das principais Universidades e Centros de Pesquisa envolvidos com estudos nesse âmbito do conhecimento.

A área de Visão Computacional é altamente multidisciplinar e caracteriza-se primordialmente pela utilização de imagens digitais associadas a técnicas de Reconhecimento de Padrões, Processamento de Imagens, Fotogrametria, entre outras. Além disso, o estudo de métodos cognitivos, de processos biológicos, processos físicos e estatísticos tem gerado soluções significativas para problemas de vital importância do mundo real.

O conjunto de técnicas oriundas desse novo campo do saber possui aplicações em diferentes áreas do conhecimento humano e com impactos relevantes nas vidas de cidadãos comuns. Entre elas, podemos citar: auxílio no diagnóstico de doenças graves a partir da análise de imagens médicas, navegação autônoma de robôs, de veículos aéreos e terrestres, biometria, sensoriamento remoto e automatização do controle de qualidade em processos industriais (inspeção industrial).

O propósito principal do Workshop de Visão Computacional (WVC) é possibilitar a integração de pesquisadores brasileiros que atuam nessa área, de modo a facilitar a apresentação, divulgação e discussão de trabalhos desenvolvidos ou em desenvolvimento, fomentar e disseminar a nucleação de novos grupos de pesquisas, assim como estimular alunos de graduação a iniciarem seus estudos nessa área por meio de ações específicas de formação que são materializadas por minicursos introdutórios. Nesse sentido, o WVC constitui-se num importante espaço de integração para a troca de experiências acadêmico-científicas, objetivando o desenvolvimento da ciência e da tecnologia brasileira nesse domínio do conhecimento.

A primeira edição do evento ocorreu em 2005 na cidade de Piracicaba, SP. Nos anos subsequentes, o evento aconteceu, respectivamente, nas cidades de São Carlos, São José do Rio Preto, Bauru e São Paulo. Apesar de ter sido, até o presente momento, realizado apenas em cidades paulistas, tem conseguido atrair trabalhos de pesquisadores de diferentes partes do país e, desse modo, está se consolidando como um evento de referência em âmbito nacional. Há interesses para que o evento expanda suas fronteiras, alcançando outros estados, assim, na Assembléia Geral realizada durante o evento, grupos de pessoas representando Universidades e Centros de Pesquisas poderão se candidatar para realizarem as próximas edições. Um histórico dos eventos já efetuados pode ser obtido a partir do **site <http://iris.sel.eesc.usp.br/wvc>**, onde é possível acessar o conjunto de informações relacionadas às edições anteriores, bem como o nível qualitativo dos respectivos programas.

O WVC é um evento científico que já está devidamente institucionalizado e tem contado com o suporte financeiro da FAPESP e da CAPES, além do apoio da SBC, das Universidades e dos Departamentos onde o evento acontece. Sua importância tem crescido no cenário nacional, sendo o único evento a tratar especificamente de pesquisas envolvendo Visão Computacional. No ano de 2010 irá alcançar a 6ª edição e será realizado na Faculdade de Ciências e Tecnologia da Universidade Estadual Paulista "Júlio de Mesquita Filho" – UNESP, localizada na cidade de Presidente Prudente. Reafirmamos os objetivos enumerados acima e esperamos contar com sua presença entre os participantes do VI WVC. Desde já nos colocamos a sua inteira disposição.

Prof. Dr. Marco Antônio Piteri
Coordenador Geral do VI WVC

piteri@fct.unesp.br
(018) 9784 7767
[Skype] marco.piteri1

Noise reduction on CT Set of Projections by Wiener Filtering and Wavelet Thresholding

Eduardo S. Ribeiro[1], Nelson D. A. Mascarenhas[1], Fernando V. Salina[2] and Paulo E. Cruvinel[3]
[1]*Federal University of São Carlos – Computer Departament*
[2]*University of São Paulo - Institute of Physics of São Carlos*
[3]*EMBRAPA – Agricultural Instrumentation*
eduardosss@gmail.com, nelson@dc.ufscar.br, fsalina@gmail.com, cruvinel@cnpdia.embrapa.br

Abstract

In this paper, we present a comparison of two techniques for noise reduction on CT set of projections. We use for filtering the Pointwise Wiener filter and thresholding of the Wavelet coefficients. We use the Anscombe transformation for noise variance stabilization. The Pointwise Wiener filter was computed with an adaptive windowing scheme for the calculation of local estimates. For the thresholding in Wavelet domain, we compare three families of wavelet bases: Daubechies, Symlets and Coiflets. We also compared four techniques for obtaining thresholds: Universal threshold, Oracle shrink, Minimax threshold and SURE threshold. For the image reconstruction stage we applied the parallel POCS algorithm. The experiments were done with one simulated phantom (Shepp-Logan) and real projections captured by a CT scanner developed by CNPDIA/EMBRAPA. The results were measured with the ISNR and SSIM criteria. In most cases, the best results were obtained with the Pointwise Wiener filter with adaptive windowing.

1. Introduction

Computerized tomography is a technique used to obtain an image of the inside of a body in a non-invasive and non-destructive manner. Since its discovery, it has been widely applied to clinical diagnosis and medical investigations. However, there are applications of CT in many other research areas, such as agriculture, engineering and biology. The tomographic data acquisition is performed by exposure of the body to the rays of the tomograph. Projections are taken from different angles around the body. The two-dimensional image is reconstructed from this set of one-dimensional projections.

Limiting the dose of radiation is a major concern in the use of CTs. In the case of tomography for clinical use, a high level of radiation to obtain the tomographic projections can cause cancer in patients [6]. In other applications it is desirable to reduce the acquisition time of tomographic data as in CT scanners used in soil science.

Low doses of radiation generates noise in the projections and consequently in the reconstructed image. To improve the image quality we can filter the tomographic projections or the image itself. Thus, a compromise between limiting the acquisition process and the quality of tomographic imaging remains.

Many researchers have studied techniques for filtering the projections or tomographic images to obtain an image with better visual quality.

In the study by Li et al [12] the filtering of tomographic projections of a clinical CT scanner was studied. 2D filtering was performed with a Bayesian estimator, where the prior knowledge was modeled with Markov random fields characterized by a Gibbs distribution.

In [13] the filtering with the method of Penalized Multiscale Least Squares (PWLS) was performed. The Wavelet transform was applied to decompose the sinogram in different levels of resolution. At each level the criterion PWLS was applied for noise reduction of the wavelet coefficients.

2. Tomographic Reconstruction

The most widely used algorithm for tomographic image reconstruction is Filtered Back Projection method (FBP), which performs the reconstruction in the frequency domain. The method is based on the Fourier slice theorem. This theorem says that the Fourier transform of a one-dimensional projection corresponds to a slice of the two-dimensional Fourier transform of the unknown image [7].

The reconstruction with the FBP algorithm displays not very satisfactory results in the presence of noise. But there are algebraic algorithms, which seek the solution in an iterative manner and show better results in the presence of noise [7]. In the reconstruction made by algebraic algorithms an image is represented by a single point in N-dimensional space. In this space each equation represents a hyperplane. When there is only one solution to these equations the intersection of all these hyperplanes is a single point, given by the solution. The algebraic reconstruction technique (ART) seeks the solution by

sequential projection on the set of linear equations, where each equation set represents a hyperplane. The simultaneous iterative reconstruction technique (SIRT) seeks a solution through the parallel projection on the hyperplanes and gives better results with noise.

In [10], ART and SIRT algorithms are considered special cases of the POCS method (Projections Onto Convex Sets), where each hyperplane is considered a convex set. In the sequential POCS algorithm when there is no single solution due the noisy projections the solution oscillates between the sets of restrictions. On the other hand, in the parallel implementation of the POCS algorithm, the solution converges to a least squares distance between the sets of possible solutions.

Filtering methods rarely eliminate completely the noise. Despite the filtering of the projections, the use of the parallel POCS algorithm results in an image with better quality. In contrast, the time of reconstruction of the parallel POCS algorithm is greater than the FBP method, because algebraic reconstruction algorithms are iterative.

3. Filtering Techniques

The predominant noise in tomographic projections is the quantum noise, which follows the Poisson distribution. This noise is due to the statistical nature of the process of emission and detection of photons. The Poisson noise is signal dependent, since its variance is equal to the mean (rate) of the Poisson distribution. Most filtering methods consider the noise as additive, ie with constant variance. There are several techniques to stabilize the variance of the noise. The Anscombe transform (equation 1) is the most widely used. It transforms the Poisson noise into additive noise with zero mean and unit variance [1]. Whereas the original signal is estimated by some method of filtering, after the completion of the Anscombe transform, the inverse Anscombe transform is given by equation 2,

$$z_i = 2\sqrt{y_i + \frac{3}{8}} \tag{1}$$

$$\hat{g}_i = \frac{1}{4} z_i^2 - \frac{1}{8} \tag{2}$$

where y represents the noisy signal and z represents the signal in the Anscombe domain.

The filtering techniques are applied in the Anscombe domain. These techniques will be discussed in following sections.

3.1 Wiener Filter

The Wiener filter is optimal to minimize the mean square error between the estimated signal and the original signal. There are several implementations of this filter. We will analyze the pointwise Wiener filter defined by equation 3 [8],

$$\hat{g} = \mu_g + \frac{\sigma_g^2}{\sigma_g^2 + \sigma_n^2}(y - \mu_y) \tag{3}$$

where y is noisy signal, μ_g is the mean of the original signal, μ_y is the mean of the noisy signal and σ_g^2 is the variance of the original signal. We know that the noise variance σ_n^2 is one in the Anscombe domain.

To compute the pointwise Wiener filter it is necessary to estimate the mean and variance at each point of the signal. As we do not have access to the original signal, a preliminary estimate of the signal can be made through a mean filter. After this initial estimate is made, the sample mean and sample variance are calculated.

The way to perform the calculation of local estimates significantly influences the outcome of filtering. We can use a fixed or an adaptive window for the computation of local estimates.

In the adaptive windowing, few points are considered in regions with edges for the calculation of local estimates. In flat regions of the signal, more points can be considered for the computation of the estimates. In this work we use a scheme for the adaptive windowing-based method based on the work of Rabbani [9].

Rabbani's method consists of analyzing the relationship between the variance of the original signal and the variance of the noisy signal (equation 4) and an approach for calculating the gradient (equation 5).

$$\alpha = \frac{\sigma_g^2}{\sigma_y^2} \tag{4}$$

$$r = \frac{|Mn - M| - |Ms - M|}{|Mn - Ms|} \tag{5}$$

In equation 5, M represents the central point, Ms are its two neighbors points of the left and Mn are its two neighbors points on the right.

The two indicators, α and r, are compared with thresholds to determine if the projection point features an edge or a flat region. We will use t as a threshold for α and T as a threshold r. When $\alpha < t$, we can say that it is an area of moderate activity signal and the calculation of local estimates is done with a window of 5 elements. When $\alpha > t$, we also analyze the value of r.

When $r > T$, there is an indication of local roughness, but no edge. In this case we still use the window with 5 elements to calculate the estimates. But when we find $\alpha > T$, there is evidence of an edge. In this case, the local estimates are computed with 3 window elements. Experimentally we choose $t = 0.3$ and $T = 0.2$.

3.2 Noise Reduction using Wavelets

The wavelet transform performs the analysis of the data variables in the time and frequency domains. The discrete wavelet transform represents a signal in terms of displacements functions φ and scale functions ψ.

A characteristic of data representation in the wavelet domain is the multi-scale analysis. The signal can be decomposed into several levels that can be analyzed independently. Using the orthogonal wavelet transform a signal can be decomposed according to equation 6 [2].

$$s(l) = \sum_k c_{J,k}\phi_{J,l}(k) + \sum_{j=l}^{J}\sum_k w_{j,k}\psi_{j,l}(k) \quad (6)$$

where

$$\psi_{j,k}(x) = 2^{-j}\psi\left(2^j x - l\right) \quad (7)$$

$$\phi_{j,k}(x) = 2^{-j}\phi\left(2^{-j} x - l\right) \quad (8)$$

The noise reduction in wavelet domain is done by applying a threshold on the coefficients. There are two ways of applying the threshold: hard thresholding and soft thresholding. The hard thresholding is given by equation 9 and the soft thresholding is given by equation 10, where λ is the threshold value.

$$p_{hard}(x) = \begin{cases} x, & |x| < \lambda \\ 0, & othersiwe \end{cases} \quad (9)$$

$$p_{soft}(x) = \begin{cases} x - \lambda, & x \geq \lambda \\ x + \lambda, & x \leq -\lambda \\ 0, & otherwise \end{cases} \quad (10)$$

We analyzed four techniques to obtain the threshold value. The first technique is the Universal threshold, which is defined by equation 11, where N is the sample size and σ is the standard deviation of noise [4,5].

$$\lambda = \sqrt{2\log N}\sigma \quad (11)$$

The second threshold (Oracle shrink or Oracle threshold) is optimal under the criterion of mean square error. It is assumed that the original signal is known. The threshold value is obtained by minimizing equation 12 [4].

$$\lambda = \arg\min\{\| y_\lambda - g \|^2\} \quad (12)$$

Donoho and Johnstone proposed the Minimax threshold [3]. This threshold differs from Universal threshold because it does not implies into an excessive smoothing. The Minimax threshold keeps the abrupt changes of the signal. The value of the threshold t is given when it reaches the value given by equation 14,

$$\lambda = \inf_t \sup_y \left\{ \frac{R_t(y)}{n^{-1} + R_{oracle}(y)} \right\} \quad (13)$$

where y are the Wavelet coefficients, $R_t(d) = E[y_t - y]^2$, and $R_{oracle}(d)$ can be defined by equation 14 or 15.

$$R_{oracle}^{DPL}(y) = \min(y^2, 1) \quad (14)$$

$$R_{oracle}^{DLS} y = \frac{y^2}{y^2 + 1} \quad (15)$$

The SURE threshold was proposed by [5]. The choice of the threshold follows the principle of Stein's Unbiased Risk Estimate (SURE). The choice of the threshold consists of finding a value that minimizes the risk function described by equation (17),

$$\lambda_{SURE} = \arg\min\{SURE(\lambda)\} \quad (16)$$

where,

$$SURE(\lambda) = \left[\left(\frac{1}{N}\| y_\lambda - y \|^2\right) - \sigma^2\right] + \left[2\lambda^2 \frac{N - N_0}{N}\right] \quad (17)$$

y_λ are the coefficients after the application of Wavelet threshold, N is the number of coefficients, N_0 is the number of zero coefficients after applying the threshold, and σ^2 is the variance of the noise.

4. Experiments

For the experiments we used several sets of projections. We used the simulated Shepp-Logan phantom and projections obtained by a mini CT scanner developed by the National Center for Research and Development of Agricultural Instrumentation of the Brazilian Agricultural Research Company (CNPDIA-EMBRAPA). For each phantom, two sets of projections were captured. For the first, each point was obtained with 3 seconds of exposure to the rays of the CT scanner; for the second, the exposure was 20 seconds. The projections of 3 seconds of exposure are noisy. This is due to low photon counting and we will filter these projections. The projections with 20 seconds of exposure have a higher photon count and the noise level was very low. The reconstructed image from these projections will be used for the comparison of filtering methods.

The filtering evaluation was performed after the image reconstruction, considering the following criterion: ISNR (Improvement in Signal-to-Noise Ratio) and SSIM (Structural Similarity Index). Equation 17 shows the formulation of the ISNR criterion, where y is the noisy image, g is the original image and $\hat{g}$ is the estimated image. The test results in 0 when the estimated image is equal to the noisy image and results in infinity when the estimated image is equal to the original image.

$$ISNR = 10\log\frac{\sum_j (y_j - g_j)^2}{\sum_j (g_j - \hat{g}_j)^2} \quad (17)$$

The SSIM criterion is given by equation 18. It is the combination of three indicators: the luminance, contrast and structural similarities. μ_g and μ_g are the means of the original image and estimated image. σ_g^2 and σ_g^2 are the variances of the original image and estimated image. $\sigma_{\hat{g}g}^2$ is the correlation between g and $\hat{g}$. C1 C2 and C3 are constants that stabilize each term. Usually the criterion works well when these constants are 0. The value of SSIM is given between -1 and 1, the value 1 is achieved only when the estimated image is equal to the original image [11].

$$SSIM = \left(\frac{2\mu_{\hat{g}}\mu_g + C_1}{\mu_{\hat{g}}^2 + \mu_g^2 + C_1}\right)\left(\frac{2\sigma_{\hat{g}}\sigma_g + C_2}{\sigma_{\hat{g}}^2 + \sigma_g^2 + C_2}\right)\left(\frac{2\sigma_{\hat{g}g} + C_3}{\sigma_{\hat{g}}\sigma_g + C_3}\right) \quad (18)$$

In the experiments we use three families of basis: Daubechies, and symlets coiflets. For the filtering using the Wavelet thresholding we selected one basis from each family through experimental tests. We also chose two levels of decomposition and the use of soft thresholding.

The projections of the Shepp-Logan phantom were obtained by applying the Radon transform on the image of the phantom. On the projections set (sinogram) we inserted Poisson noise. The Radon transform was performed to obtain a sinogram with size 128x128.

Table 1 shows the results of the measurement error of the reconstructed image with the filtered sinogram. The pointwise Wiener filter achieved better results with adaptive windowing. In projections of the Shepp-Logan phantom the Universal threshold showed the best performance for the thresholding of wavelets coefficients. The Sym10 basis displayed the best results.

Table 1 - Error measures of reconstructed images from the filtered projections of Shepp-Logan phantom.

Filter	*Window/ Threshold*	*ISNR*	*SSIM*
Pointwise Wiener Filter	3	1.9101	0.35870
	5	1.7351	0.39237
	3 e 5	**3.5987**	**0.40970**
Wavelet – Db12	Oracle	2.6730	0.34947
	Universal	**2.7487**	**0.35258**
	Minimax	2.7176	0.35013
	SURE	1.8949	0.34347
Wavelet – Coif3	Oracle	1.4258	0.34348
	Universal	**2.1487**	**0.34895**
	Minimax	1.4115	0.34602
	SURE	0.5656	0.33709
Wavelet – Sym10	Oracle	**3.1698**	0.35233
	Universal	3.1229	**0.35374**
	Minimax	2.6255	0.35085
	SURE	1.1135	0.34224

Figure 2 shows some reconstructed images with filtering the projections with the techniques that have shown better results.

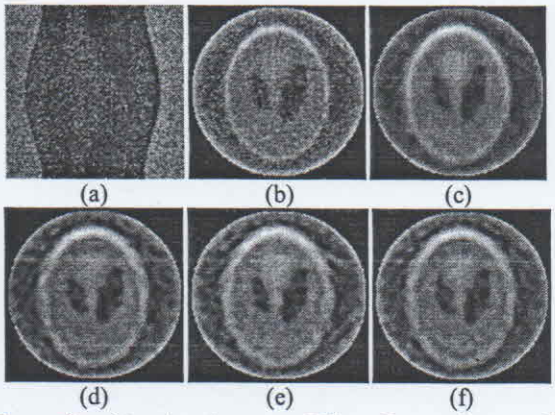

Figure 2 – (a) noisy sinogram of Shepp-Logan phantom, (b) reconstructed image from this sinogram, (c) reconstructed image from the filtered sinogram with pointwise Wiener filter and adaptive windowing, (d) sinogram filtered with wavelet thresholding - Sym10 basis and universal threshold, (e) db12 basis and universal threshold, (f) coif3 basis and universal threshold.

Three phantoms were used to obtain the projections of the CT scanner developed by CNPDIA-EMBRAPA. The phantoms have homogeneous, symmetrical and asymmetrical composition.

The first phantom was built with a plexiglass cylindrical structure with water (H_2O) inside. The set of projections of this phantom has dimensions of 79x79. Each projection has 79 points and 79 projections were obtained.

Table 2 shows the results of the measurement error of the reconstructed image from the filtered projections. In this phantom the wavelet thresholding with Db12 and Sym10 basis surpassed the results of the Wiener filter. Under the criterion ISNR the best threshold was the Minimax threshold; however the criterion SSIM indicates the Universal threshold as the best. Figure 3 shows the reconstructed images after filtering the projections.

Table 2 – Error measures of reconstructed images from the filtered projections - homogeneous phantom.

Filter	*Window/ Threshold*	*ISNR*	*SSIM*
Pointwise	3	2.0726	0.24357
	5	**2.2442**	0.25668

Wiener Filter	3 e 5	2.1659	**0.26297**
Wavelet – Db12	Oracle	2.3076	0.29158
	Universal	2.4391	**0.29666**
	Minimax	**2.6277**	0.28871
	SURE	2.5047	0.27009
Wavelet – Coif3	Oracle	1.6875	0.25946
	Universal	**1.6959**	**0.26162**
	Minimax	1.6889	0.24717
	SURE	1.6833	0.22756
Wavelet – Sym10	Oracle	2.1225	0.29466
	Universal	2.1639	**0.29828**
	Minimax	**2.5204**	0.28226
	SURE	2.1912	0.25100

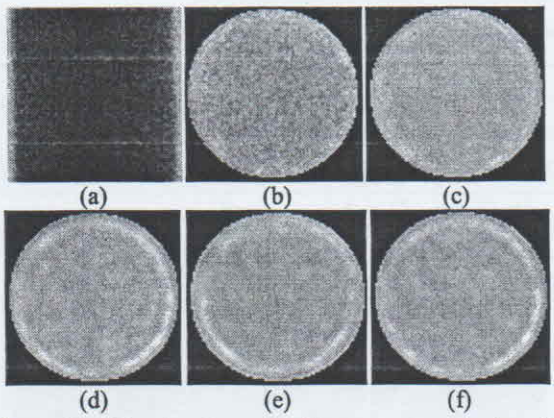

Figure 3 – (a) noisy sinogram of homogeneous phantom, (b) reconstructed image from this sinogram, (c) reconstructed image from the filtered sinogram with pointwise Wiener filter and adaptive windowing, (d) filtered sinogram with wavelet thresholding - Db12 basis and minimax threshold, (e) coif3 basis and universal threshold, (f) sym10 basis and universal threshold.

The symmetrical phantom is composed of a cylindrical plexiglass with four holes inside symmetrically arranged. Two parallel holes were filled with aluminum (Al) and the other two were not completely, leaving air inside. The set of projections of this phantom also has a 79x79 dimension.

Table 2 shows the results of the measurement error of the reconstructed image with the filtering of the phantom symmetrical sinogram. The pointwise Wiener filter presents the best results. Filtering with the thresholding of Wavelet coefficients resulted in very similar results, and the best results were obtained with the Db12 basis and use of the Universal threshold.

Table 3 - Error measures of reconstructed images from the filtered projections - symmetrical phantom.

Filter	*Window/ Threshold*	*ISNR*	*SSIM*
	3	3.3845	0.84747
Pointwise Wiener Filter	5	2.1820	0.82658
	3 e 5	**5.3709**	**0.88644**
Wavelet – Db12	Oracle	2.5060	0.81538
	Universal	2.5814	0.81654
	Minimax	3.2064	0.82621
	SURE	**3.9305**	**0.83610**
Wavelet – Coif3	Oracle	3.7757	0.83437
	Universal	**3.8073**	**0.83590**
	Minimax	1.8868	0.81013
	SURE	0.2305	0.78566
Wavelet – Sym10	Oracle	2.8338	0.82172
	Universal	2.8960	0.82431
	Minimax	**3.4186**	**0.83461**
	SURE	1.7627	0.80670

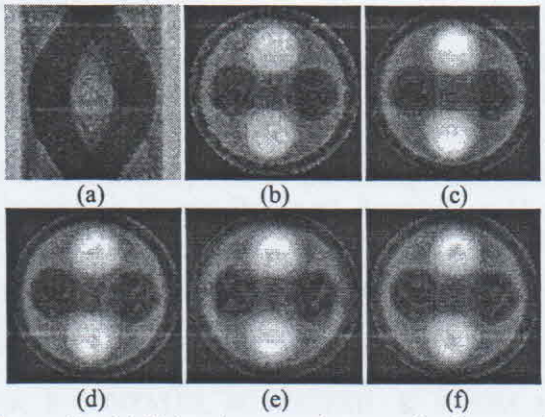

Figure 4 - (a) Noisy sinogram of symmetric phantom, (b) noisy image, (c) reconstructed image from the filtered sinogram with pointwise Wiener filter and adaptive windowing, (d) sinogram filtered with wavelet thresholding - db12 basis and SURE threshold, (e) coif3 basis and universal threshold, (f) sym10 basis and minimax threshold.

The third phantom (asymmetric) was constructed from a plexiglass cylindrical structure with ten holes in it. The holes have different diameters. The asymmetric phantom sinogram has size 100x100.

Table 4 show the results of the measurement error of filtering of the asymmetrical phantom sinogram. The pointwise Wiener filter showed the best results. Figure 5 shows the reconstructed images after the filtering of the projections.

Table 4 - Error measures of reconstructed images from the filtered projections - asymmetrical phantom.

Filter	*Window/ Threshold*	*ISNR*	*SSIM*
Pointwise Wiener Filter	3	**6.2718**	0.70479
	5	5.0834	0.70890
	3 e 5	6.0210	**0.72149**

Wavelet – Db12	Oracle	4.2005	0.70009
	Universal	4.7233	**0.70765**
	Minimax	**5.3530**	0.70607
	SURE	5.2798	0.69614
Wavelet – Coif3	Oracle	3.5545	0.68531
	Universal	3.9739	0.68434
	Minimax	4.3308	**0.68857**
	SURE	**4.7923**	0.68482
Wavelet – Sym10	Oracle	4.1445	0.70280
	Universal	4.1556	**0.70408**
	Minimax	4.6148	0.69835
	SURE	**4.6180**	0.68676

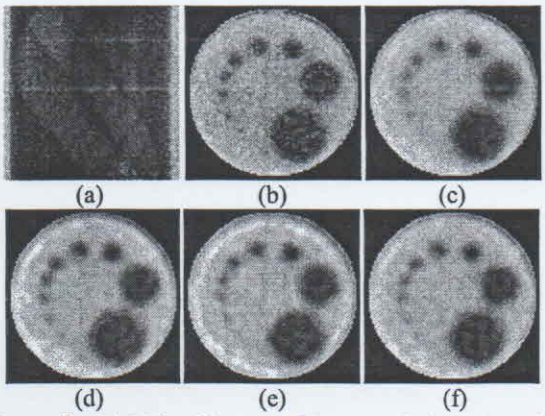

Figure 5 - (a) Noisy sinogram of asymmetrical phantom, (b) noisy image, (c) reconstructed image from the filtered sinogram with pointwise Wiener filter and adaptive windowing, (d) sinogram filtered with wavelet thresholding – db12 basis and universal threshold, (e) Coif3 basis and Minimax threshold, (f) Sym10 basis and Universal threshold.

5. Conclusions

The pointwise Wiener filter in most cases showed the best results. The only exception was with the homogeneous phantom in which the Wavelets were better. This is because of the composition of the phantom that has no structure inside. The adaptive windowing in all cases improved the performance of the pointwise Wiener filter considering the SSIM criteria. The Wiener filter is characterized by computation of local estimates at each point to be filtered in the projection, while the Wavelet thresholding has a global dynamics in conducting Wavelet transform and obtaining the threshold.

6. References

[1] F. J. ANSCOMBE, "The Transformation of Poisson, Binomial and Negative-Binomial Data", *Biometrika*, v. 35, n. 3-4, p. 246-254, 1948.

[2] I. DAUBECHIES, "*Ten Lectures on Wavelets*", Society for Industrial and Applied Mathematics, 1992, ISBN 0898712742.

[3] D. L. DONOHO, I. JOHNSTONE, "Minimax Estimation Via Wavelet Shrinkage", *Annals of Statistics*, v. 26, p. 879-921, 1998.

[4] D. L. DONOHO, I. M. JOHNSTONE, "Ideal Spatial Adaptation via Wavelet Shrinkage", *Biometrika*, v. 81, p. 425-455, 1994.

[5] D. L. DONOHO, I. M. JOHNSTONE, "Adapting to Unknown Smoothness via Wavelet Shrinkage", *American Statistical Association*, v. 90, p. 1200-1224, 1995.

[6]A. B GONZALEZ, M. MAHESH,, K. P. KIM, M. BHARGAVAN, R. LEWIS, F. METTLER, V. LAND, "Projected Cancer Risks from Computed Tomographic Scans Performed in the United States in 2007", *Archives of Internal Medicine*, v. 169, n. 22, p. 2071-2077, 2009.

[7] A. C. KAK, M. SLANEY, *Principles of Computerized Tomographic Imaging*, IEEE Press, 1988.

[8] D.T. KUAN, A. A. SAWCHUK, T. C. STRAND, P. CHAVEL, "Adaptive Noise Smoothing Filter for Images with Signal-dependent Noise", *IEEE Transactions on Pattern Analysis and Machine Intelligence*, v. 7, n. 2, p. 165-177, 1985.

[9] M. RABBANI, "Bayesian Filtering of Poisson Noise Using Local Statistics", *IEEE Transactions on Acoustics, Speech Signal Processing*, v. 36, n.6, p. 933-937, 1988.

[10] H. STARK, Y. YANG, *Vector Space Projections - A Numerical Approach to Signal and Image Processing, Neural Nets, and Optics*, John Wiley and Sons, 1998.

[11] Z. WANG, A. BOVIK, "Mean squared error: Love it or leave it?", *IEEE Signal Processing Magazine*, n. 98, p. 98-117, 2009.

[12] T. LI, X. LI, J. WANG, J. WEN, H. LU, J. HSIEH, Z. LIANG, Nonlinear sinogram smoothing for low-dose X-ray CT. IEEE Transactions on Nuclear Science ,v. 51, n. 5, p. 2505-2513 ,2004

[13] J. WANG, H. LU, J. WEN Z. LIANG, "Multiscale penalized weighted least-squares sinogram restoration for low-dose X-ray computed tomography". IEEE Transactions on Biomedical Engineering,,v. 55, n. 3, p. 1022-1031, 2008